

SOME FUNDAMENTAL EXPERIMENTS ON HIGH TEMPERATURE CREEP

By J. E. DORN

University of California, Berkeley

(Received 14th May, 1954)

SUMMARY

At high temperatures, the creep strain, ϵ , appears to be a function of a temperature (T), compensated time (t), namely $te^{-\Delta H/RT}$, and the stress. X-ray analyses and plastic properties reveal that the same structures are developed at the same values of $te^{-\Delta H/RT}$ following creep at the same stress. Thus $\epsilon = f(te^{-\Delta H/RT})$, for the same stress. When the creep rate, $\dot{\epsilon}$, is evaluated as a function of stress, σ , for the same structure

$$\dot{\epsilon} = S e^{-\Delta H/RT} \phi(\sigma)$$

where S depends on the structure and

$$S\phi(\sigma) = \begin{cases} S' e^{B\sigma} & B\sigma \geq \sim 1.4 \\ S'' \sigma^n & B\sigma \leq \sim 1.4 \end{cases}$$

Although B and n appear to be insensitive to structural changes attending creep of annealed alloys, they decrease with increasing solute additions and cold working. Transients attending loading and unloading and the coincidence of the activation energy for creep, ΔH , with that for self-diffusion suggest that high temperature creep might be ascribed to a dislocation climb process.

1. INTRODUCTION

THE principal thesis of this paper is contained in a quotation from Voltaire: "We must not say, let us begin by inventing principles whereby we may be able to explain everything; rather we must say, let us make an exact analysis of the matter and then we shall try to see, with much diffidence, if it fits in with any principle." Many theories of creep have been formulated; but the deductions based on these theories are not always in complete harmony with the experimental facts. Undoubtedly some of the assumptions on which such theories are based must be unrealistic and perhaps even fictional.

In this paper a critical analysis will be attempted on some previously published and some, as yet, unpublished experimental observations on high temperature creep. It is the author's hope that these reflections might serve to stimulate additional research which will eventually culminate in a realistic theory for high temperature creep.

2. CREEP CURVES

Three significant characteristics of the phenomenon of high temperature creep are illustrated in the typical constant true stress creep curves of Figs. 1 and 2.

(1) During loading, an initial creep strain is imposed on the specimen, the magnitude of which is determined by the stress and temperature. The subsequent portions of each creep curve exhibit three ranges; a primary stage over which the creep rate diminishes, a secondary stage yielding a minimum creep rate, and a tertiary stage, over which the creep rate increases until creep is terminated by rupture. Since, in general, the specimen does not exhibit local plastic deformation

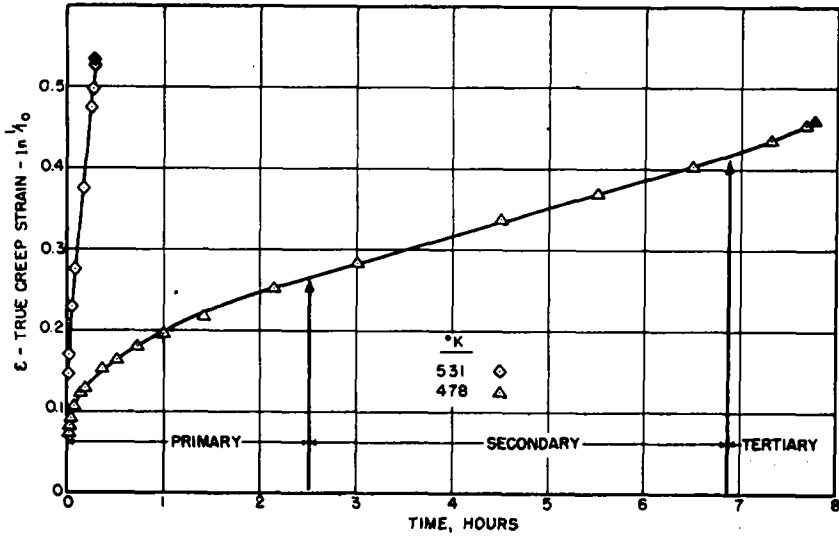


Fig. 1. Creep curves of high purity aluminium under a constant true stress of 3,000 psi.

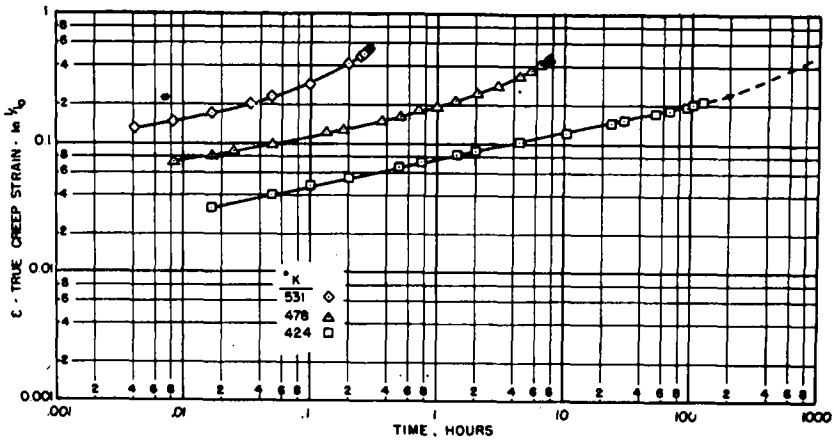


Fig. 2. Creep curves of high purity aluminium under a constant true stress of 3,000 psi.

until creep is well within the tertiary stage, the observed changes in the creep rate cannot be ascribed to changes in any of the externally controlled variables of the test. Assuming that the structure of the specimen had remained constant throughout the creep process, as it does during viscous flow of a Newtonian liquid, the creep rate should also have remained constant in a constant true stress constant

temperature test. Consequently the observed changes in the creep rate must arise from the structural changes that occur during creep. (The original investigations of WOOD and WILMS 1949; WOOD, WILMS and RACHINGER 1951 as well as those of SERVI and GRANT (1951), WYON and CRUSSARD (1951), GREENOUGH

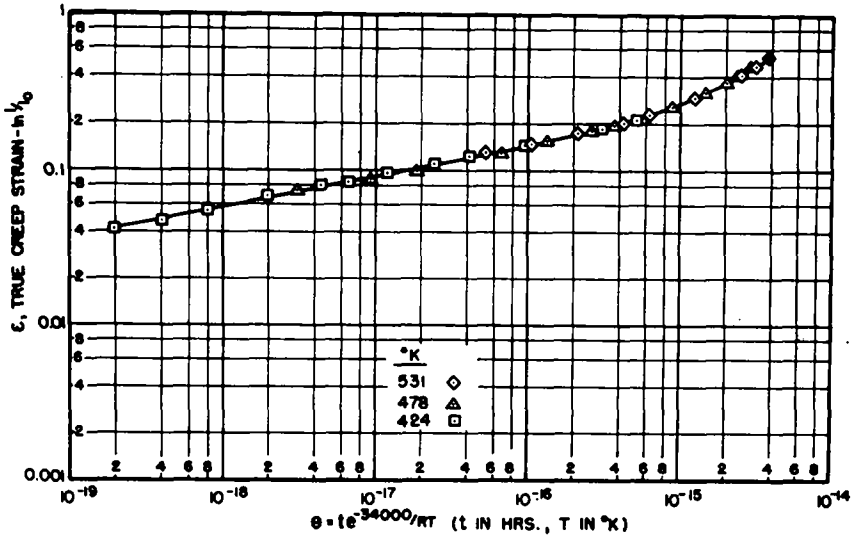


Fig. 8. Creep strain as a function of the temperature compensated time for a constant true stress of 3,000 psi.

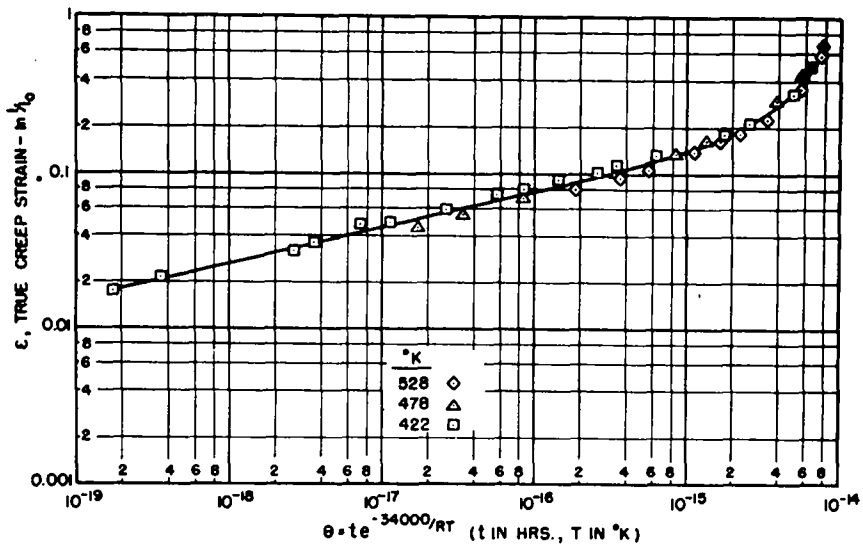


Fig. 4. Creep strain as a function of the temperature-compensated time for a constant load of 2,000 psi. (Data of SHERBY and DORN 1958).

and SMITH (1950), and SHERBY and DORN (1958) have served to identify those structural changes which are directly detectable by metallographic and X-ray diffraction techniques.)

(2) The creep rate increases rapidly with an increase in test temperature, suggesting that the creep rate is controlled by some process involving thermal activation.

(3) When the total creep strains are plotted as a function of the logarithm of the time under test (vide Fig. 2), the creep curves for the same stress and different temperatures are identical excepting for parallel displacements along the time axis. Consequently the same total creep strains are obtained for identical values of

$$\ln t + \psi(T)$$

where t is the duration of the test and ψ is some function of the temperature T . But if the rate-controlling process be one of thermal activation, the function $\psi(T)$ might be replaced by $-\Delta H/RT$, where ΔH is the activation energy and R is the gas constant. Under such assumptions the total creep strain, ϵ , would be given by the functional relationship

$$\epsilon = f(te^{-\Delta H/RT}) = f(\theta), \quad \sigma = \text{constant} \quad (1)$$

In this event the activation energy for creep could be determined from two creep tests conducted under the same stress at two different temperatures. If the times to reach the same strains at temperatures T_1 and T_2 are t_1 and t_2 respectively,

$$t_1 e^{-\Delta H/RT_1} = t_2 e^{-\Delta H/RT_2} \quad (2)$$

and ΔH can be evaluated. Knowing ΔH , the creep strains can now be plotted as a function of θ . The data recorded in Fig. 3 confirm the validity of equation 1. As revealed by the data recorded in Fig. 4, (1) is also applicable to constant load creep data. The only difference between constant load and constant true stress data arises from appropriate differences in the form of the function f .

It was considered possible that the coincidence of the $\epsilon - \theta$ curves for creep over a range of temperatures at constant stress (or load) might have been accidental and therefore of limited significance and import. But the excellence of the agreement between the $\epsilon - \theta$ curves over a series of temperatures and various stresses suggested that these correlations might have some fundamental origin. In view of the dependence of the creep rate on the structure, the basic reason for the observed correlations might be sought in the possible identity of structures obtained during creep under a given stress at the same values of θ independent of the test temperature. In order to test this concept a series of creep tests were made on the same coarse-grained high purity aluminium from which the constant load creep data of Fig. 4 were obtained. The tests were conducted at three temperatures (422, 477 and 528°K) under the same constant load of 2,000 psi. Specimens were removed from test at true strains of 0.082, 0.14, 0.22 and at fracture for each temperature and then cooled rapidly to room temperature for examination:

(1) The X-ray back-reflection Debye-Scherrer diagrams of Fig. 5 reveal that the X-ray patterns are somewhat sensitive to the creep strain and, within the scatter inherent in the X-ray sampling, approximately the same patterns are obtained at the same creep strains independent of the temperature of test. According to the correlations recorded in Fig. 4, therefore, almost identical structures are obtained at the same values of θ for creep under the same load.

(2) Metallographic examinations also confirmed the nominal identity of

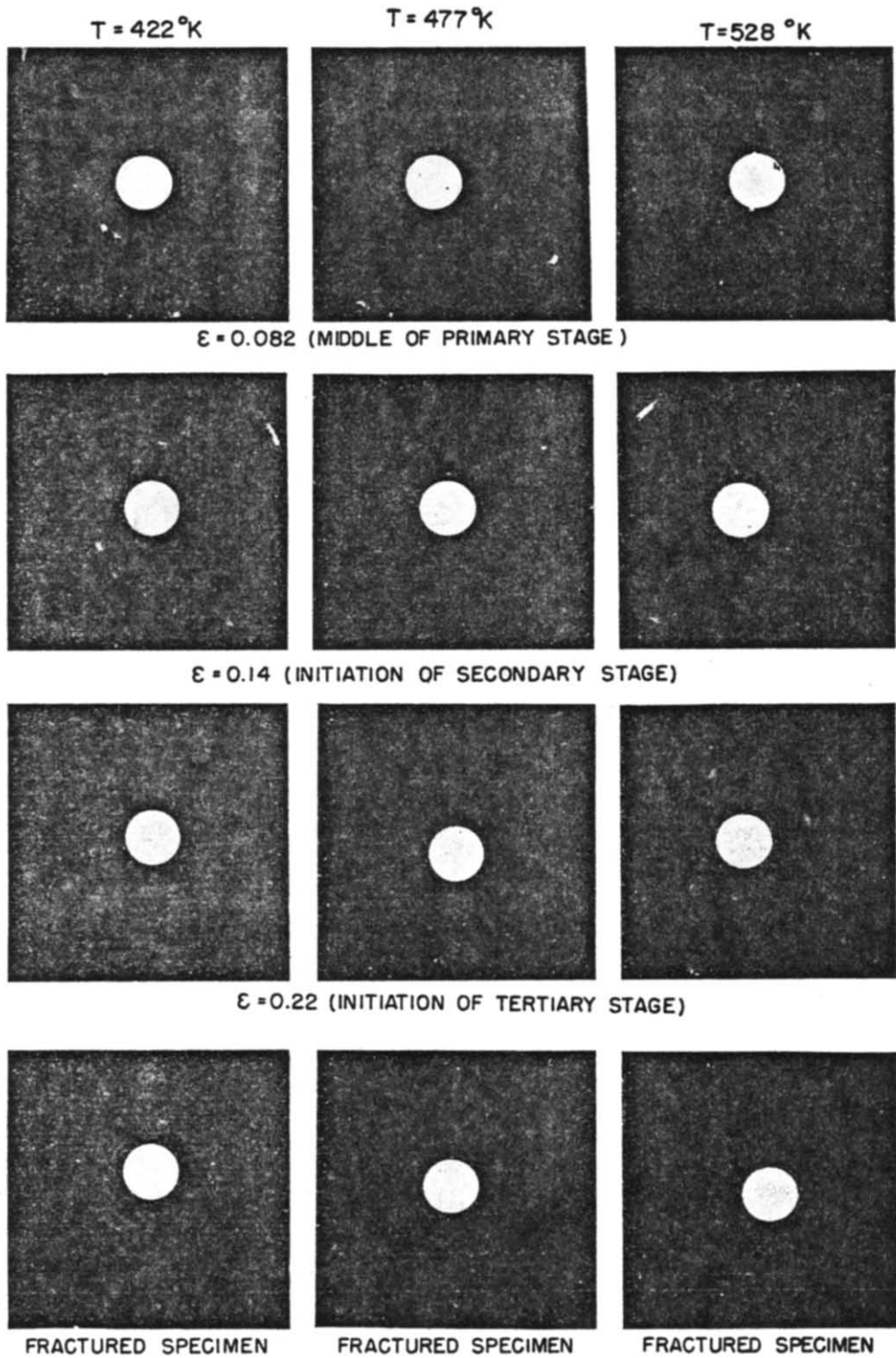


Fig. 5. X-ray back reflection photographs of high purity aluminium under a constant load of 2,000 psi for various temperatures as a function of strain.

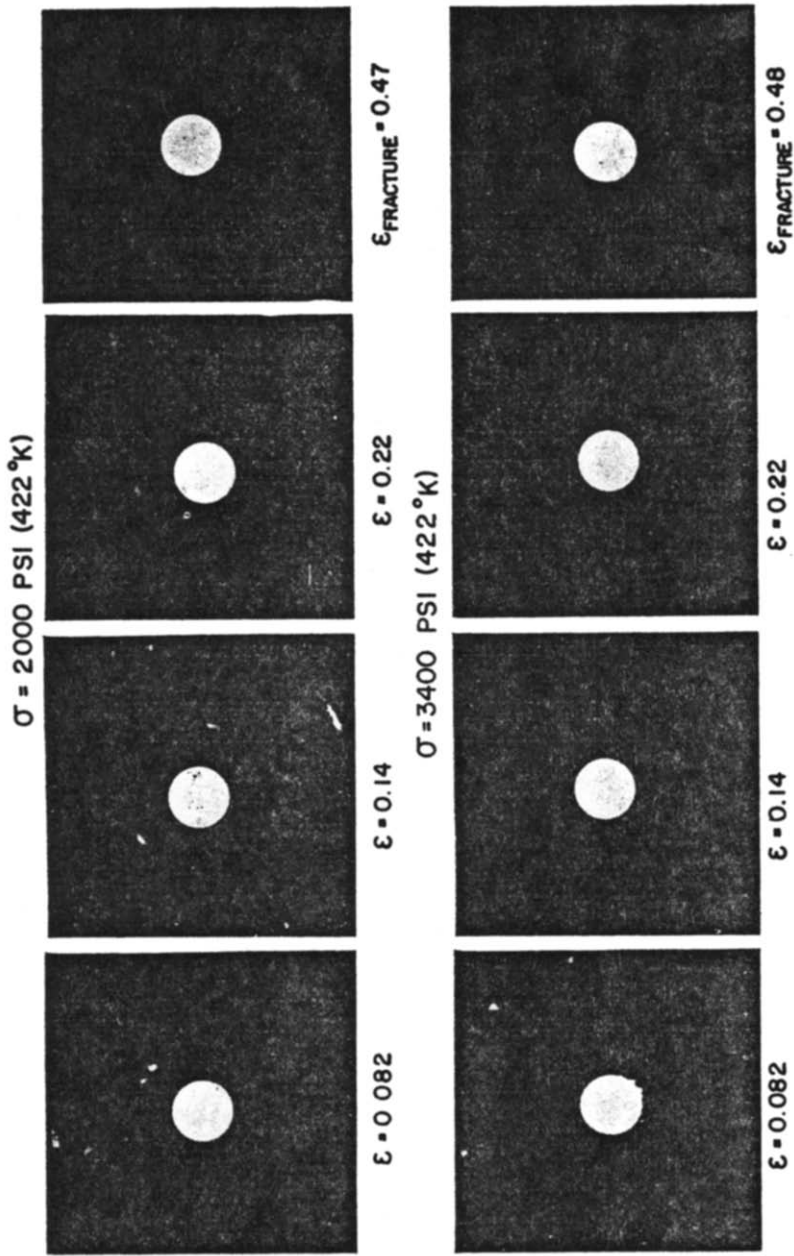


Fig. 6. X-ray back reflection photographs of high purity aluminium for two different stresses as a function of the strain.

structures at the same values of ϵ and therefore θ . At $\epsilon = 0.082$ the metallographic structures exhibited approximately the same evidence of extensive deformation banding independent of test temperature in harmony with the short diffuse arcs in the X-ray patterns arising from bending and distortions of the grains. At $\epsilon = 0.22$, however, the metallographic structures exhibited approximately the same extensive subgrain formation independent of test temperature in complete harmony with the extensive polygonization shown by the greater Debye-Scherrer arcs composed of sharp reflections arising from a series of nearly perfect subgrains. At the intermediate strains almost identical intermediate structures were obtained independent of the test temperature.

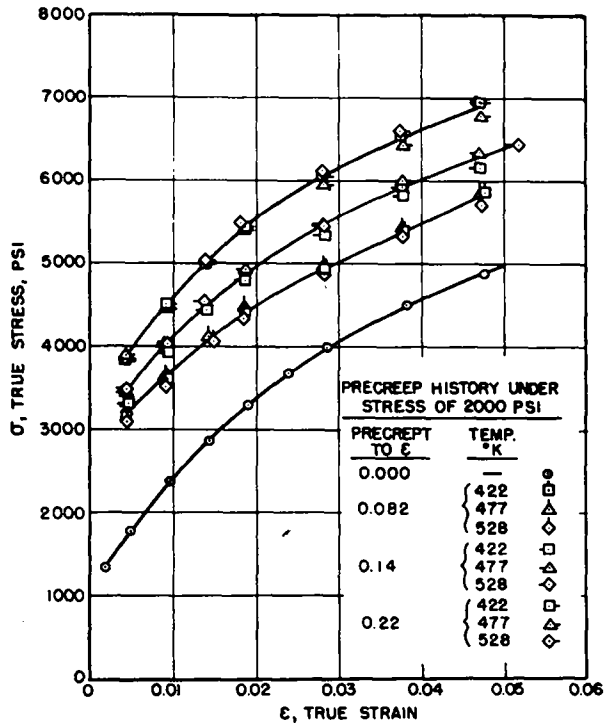


Fig. 7. Tensile properties at 298°K following creep under a constant load of 2,000 psi to strains indicated above. (Data of SHERBY and DORN 1953).

(3) Both X-ray and metallographic examination support the thesis that identical structures are obtained for the same values of ϵ or θ in a constant stress (or load) creep test, independent of the test temperature. But sampling difficulties and insensitivity inherent in these techniques suggested that a more definitive quantitative test of this concept be made; this was deemed particularly necessary inasmuch as only certain gross structural details can be revealed by X-ray diffraction and metallographic techniques. Since the plastic properties of metals are highly structure-sensitive, atmospheric temperature stress-strain curves following identical creep strains were selected for this test. As shown in Fig. 7, the stress-strain curves were sensitive to the previous creep history; and the same stress-strain curves were obtained following identical creep strains under the same

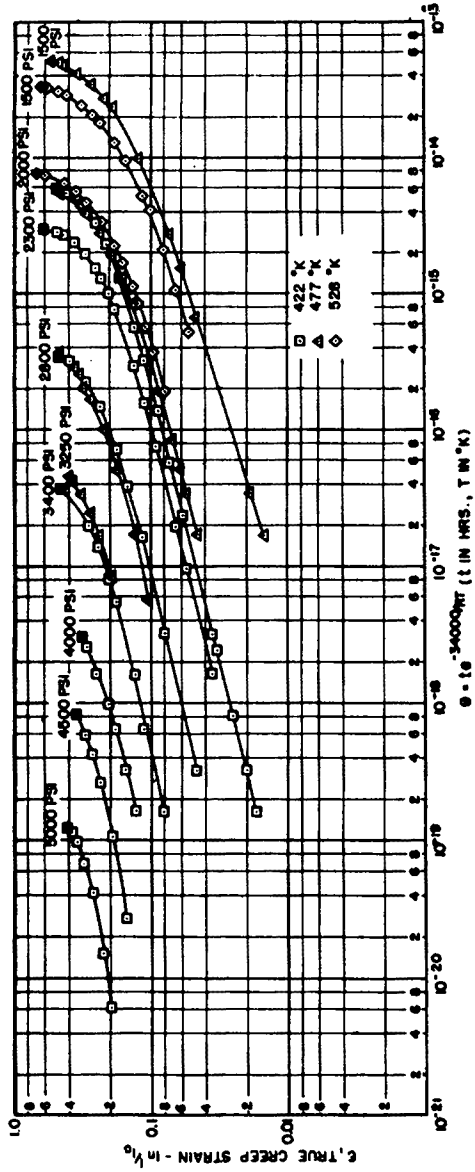


Fig. 8.

stress, independent of the test temperature. Consequently the validity of equation 1 arises from the identity of the total structure at equal values of θ and ϵ in a constant stress creep test, independent of the test temperature.

An increase in stress causes an increase in the initial strain and the subsequent creep rate, as shown by the data recorded in Fig. 8. These data also reveal that

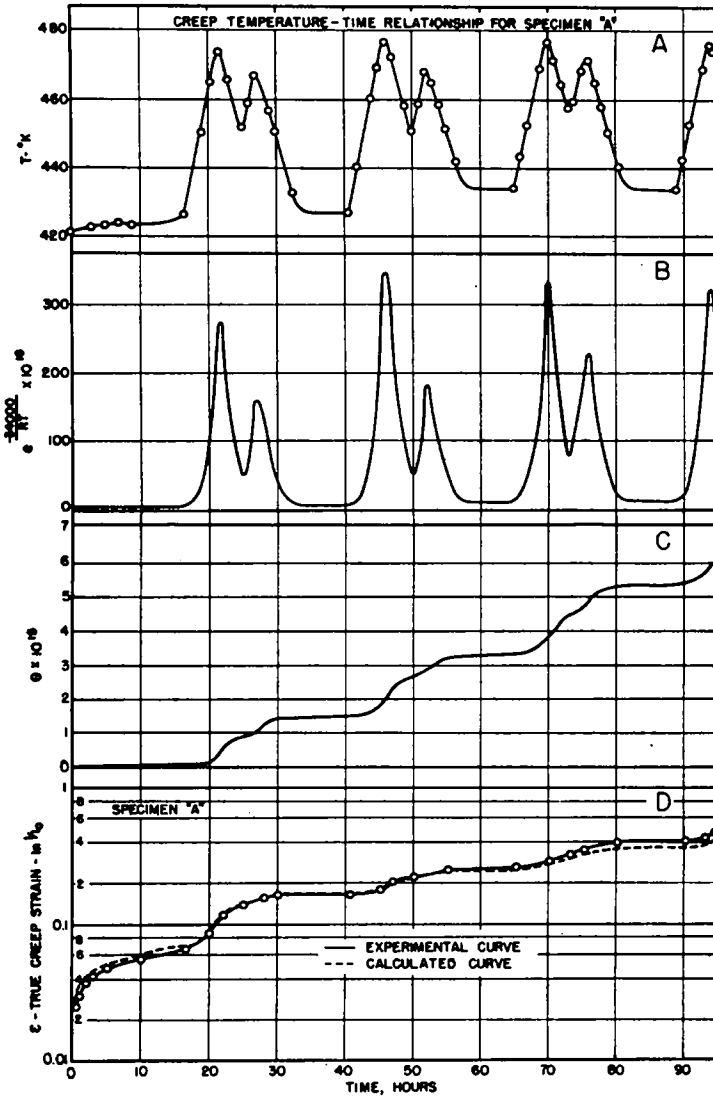


Fig. 9. Creep at a constant load of 2,000 psi under variable temperature conditions.

the activation energy for creep is insensitive to differences in the stress. As shown by the back-reflection Debye-Scherrer photograms of Fig. 6, creep to the same strain under a higher stress resulted in more diffuse arcs and finer subgrain sizes. Metallographic examination revealed more extensive deformation banding over the first portion of the creep curve at the higher stress, followed over the last

portion of the creep curve at higher stress by finer polygonized subgrain sizes. These observations suggest that the substructures developed during creep at higher stresses appear never to coincide with those developed at any strain during creep at lower stresses.

3. DEDUCTIONS BASED ON EQUATION (1)

Several deductions follow directly from equation (1).

1. *Creep under Variable Temperature.* For constant stress (or constant load) creep under conditions where the temperature is varied with time, the evaluation of θ can be generalized according to

$$\theta = \int_0^t e^{-\Delta H/RT} dt \tag{3}$$

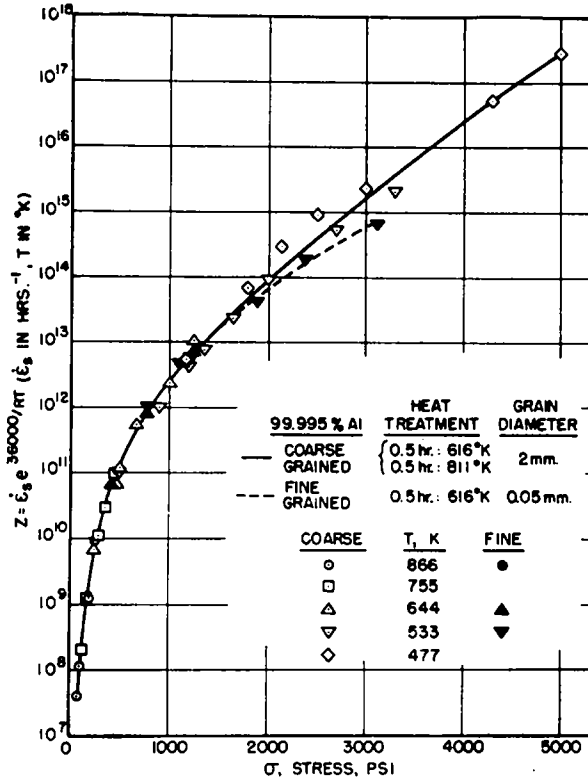


Fig. 10. Correlation between stress and the Zener-Hollomon parameter for high purity aluminium. (Data from SERVI and GRANT 1951).

which reduces to $\theta = te^{-\Delta H/RT}$ for constant temperature creep. Fig. 4 gives the $\epsilon - \theta$ curve of high purity Al under a constant load of 2,000 psi illustrating that ΔH is about 84,000 cal/mole. When the temperature is varied according to cut A of Fig. 9, the solid creep curve of cut D of Fig. 9 is obtained for a constant load of 2,000 psi. In cut B is shown the value of $e^{-\Delta H/RT}$ as a function of time from which the θ values shown in cut C are obtained by the graphical integration

suggested by (8). The strains corresponding to the calculated values of θ were obtained from the constant temperature $\epsilon - \theta$ curve of Fig. 4 and plotted as a function of time in the broken curve of cut *D* of Fig. 9. The good agreement between the calculated and experimental curves attests the validity of this method of prediction.

2. *Zener-Hollomon Parameter.* According to equation (1), the creep rate is given by

$$\dot{\epsilon} = \left(\frac{\partial f}{\partial \theta}\right) \left(\frac{d\theta}{df}\right) = f'(\theta) e^{-\Delta H/RT}, \quad \sigma = \text{constant.} \quad (4)$$

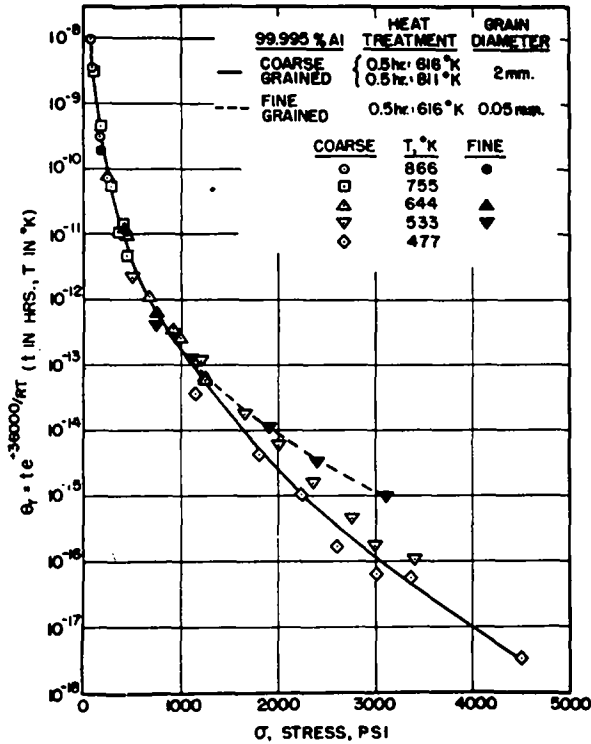


Fig. 11. Correlation between stress and θ at rupture for high purity aluminium. (Data from SERVI and GRANT 1951).

Therefore, at the secondary creep rate, designated by subscripts "s,"

$$\dot{\epsilon}_s e^{\Delta H/RT} = f(\theta_s), \quad \sigma = \text{constant.} \quad (5)$$

But as shown by (1) as well as the data recorded in Figs. 3 and 4, θ_s has the same value independent of temperature for the same stress. As the stress is increased, however, θ_s decreases, whence θ_s is a function of the stress. Consequently

$$Z = \dot{\epsilon}_s e^{\Delta H/RT} = F(\sigma) \quad (6)$$

where *Z* is the well-known Zener-Hollomon parameter (ZENER and HOLLOMON 1944). A typical correlation of *Z* as a function of σ is shown in Fig. 10. The ΔH obtained by this method agrees well with that obtained from $\epsilon - \theta$ data.

8. *Stress-Rupture.* Assuming that the strain damage leading to rupture at a given stress is dependent only on the strain to rupture, the value of θ_r at rupture should be the same for all tests under the same stress independent of temperature. This conclusion is verified by the data of Figs. 8 and 4 where the termini of the

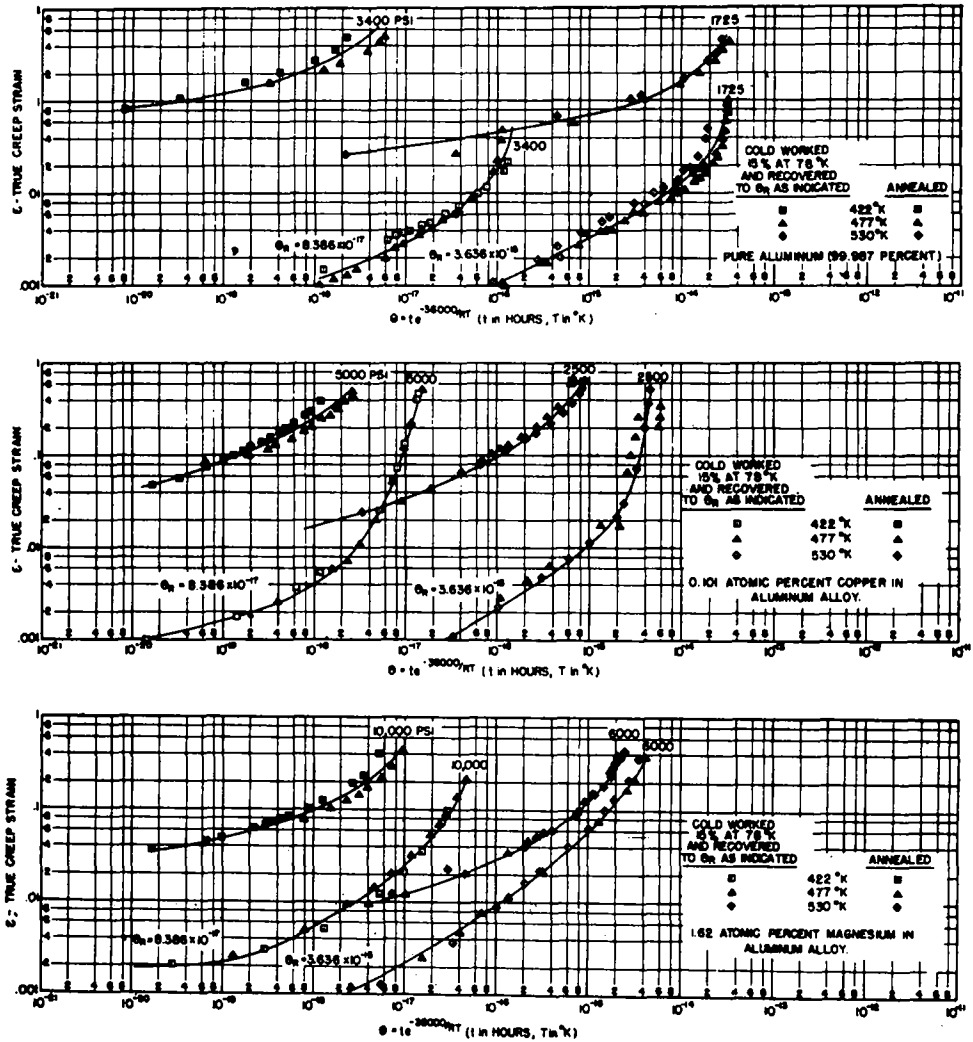


Fig. 12. Correlation of creep strain-time data for annealed and cold-worked states of dilute aluminium alloys by means of the relation $\epsilon = f(\theta_r)$ at constant load. (Data of FRENKEL, SHERBY and DORN 1953).

$\epsilon - \theta$ curves for each temperature are represented by the solid points shown on the graph. Consequently stress-rupture should obey the functional relationship (ORR, SHERBY and DORN 1954a)

$$\theta_r = t_r e^{-\Delta H / RT} = G(\sigma) \tag{7}$$

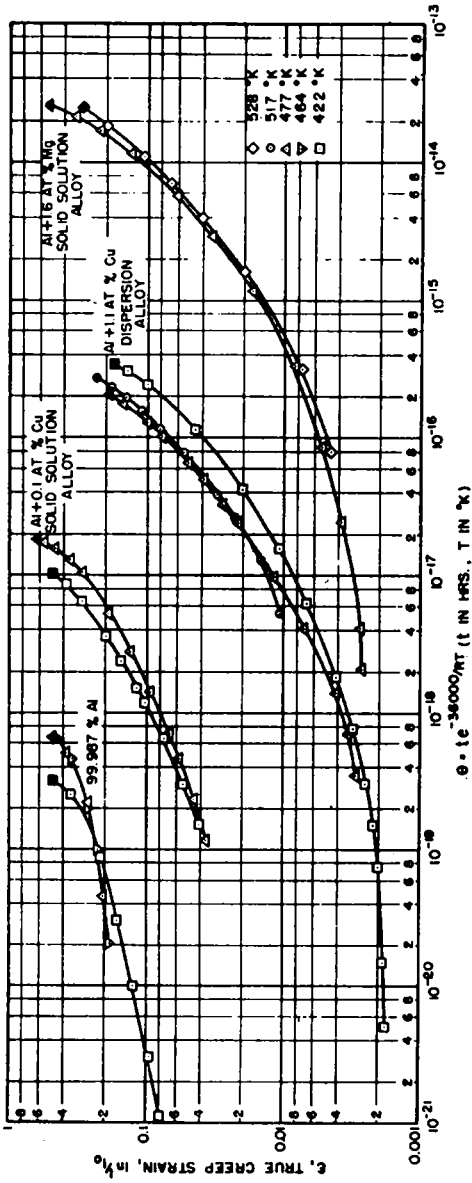


Fig. 18. Correlation of creep strain-time data for aluminum and dilute aluminum alloys by means of the relation for a constant load of 4,000 psi. (Data of Sherry and Dorn 1953, 1952; and Giedt, Sherry and Dorn 1953).

A typical example of the validity of this relationship is given in Fig. 11. Again the activation energy so obtained agrees well with those obtained from $\epsilon - \theta$ and $Z - \sigma$ types of data.

4. ACTIVATION ENERGY FOR CREEP

The methods of analyses described above are not universally applicable to all types of creep data. First they apply only when the temperature is above that for rapid crystal recovery (about one-half of the melting temperature for high purity metals). Creep data obtained at lower temperatures do not correlate with the higher temperature creep data (SHERBY and DORN 1952), suggesting that two alternate mechanisms for creep might exist, one predominating at the higher

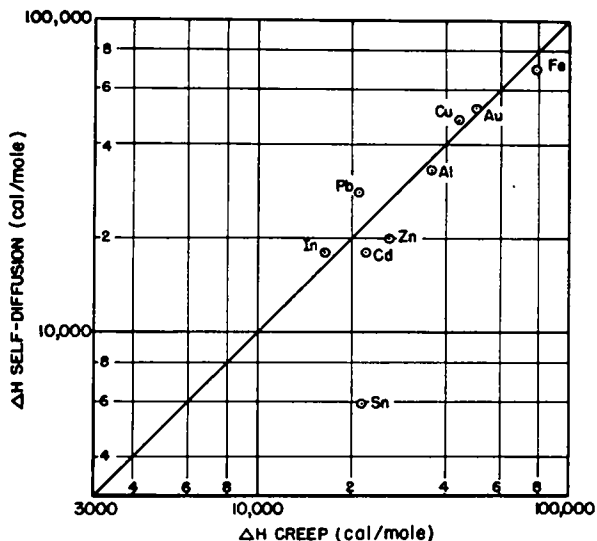


Fig. 14. Correlation between the activation energies for creep and self-diffusion.

temperatures and the other predominating over the lower ranges of temperature. Secondly the analyses described above are invalid when applied to thermally unstable systems such as precipitation hardened alloys. Such failures are ascribable to the possibility that the structures developed in these alloys following creep at a given stress are not simple functions of a single θ parameter. It is suspected that these simple correlations might not be applicable over the entire range of binary alpha solid solutions wherein two activation energies might be operative.

Within the limits of validity of (1), however, ΔH appears to be insensitive to temperature (vide Fig. 10), stress (vide Figs. 8 and 10), strain and the structure developed during creep of annealed metals (vide Figs. 3 and 4), cold worked state (FRENKEL, SHERBY and DORN 1953) (vide Fig. 12), grain size (vide Fig. 10), minor alloying additions (SHERBY and DORN 1952) (vide Fig. 13), and relatively stable dispersions of hard intermetallic compounds in dilute alpha solid solution matrices (GIEDT, SHERBY and DORN 1953) (vide Fig. 13). Since ΔH appears to be a structure-sensitive property it might be assumed that ΔH for creep of relatively pure metals approaches that of the elements.

TABLE 1.
Activation Energy for Creep.

Atomic No.	Metal	Type of Correlation	ΔH (cal/mole)	Reference	
4	Be (99.7%)	$\theta_r - \sigma$	65,000	KAUFMAN, GORDON and LILLIE (1950)	
12	Mg (99.98%)	$\epsilon - \theta$ $Z - \sigma$	31,000	ROBERTS (1958)	
18	Al (99.99%)	$\epsilon - \theta$ $Z - \sigma$ $\theta_r - \sigma$	34,000 to 36,000	SHERBY and DORN (1952); ORR, SHERBY and DORN (1954a)	
	Al-Mg Solid Solution Alloy (1.6% Mg)	$\epsilon - \theta$ $Z - \sigma$ $\theta_r - \sigma$	36,000	SHERBY and DORN (1952); ORR, SHERBY and DORN (1954a)	
	Al-Cu Solid Solution Alloy (0.1% Cu)	$\epsilon - \theta$ $Z - \sigma$ $\theta_r - \sigma$	36,000	SHERBY and DORN (1952); ORR, SHERBY and DORN (1954a)	
	Al-Cu Dispersion Alloy (1.1% Cu)	$\epsilon - \theta$ $Z - \sigma$ $\theta_r - \sigma$	36,000	GIEDT, SHERBY and DORN (1958)	
	Al (99.99%)	$Z - \sigma$ $\theta_r - \sigma$	36,000	SERVI and GRANT (1951)	
	22	Ti (99.6%)	$\theta_r - \sigma$	60,000	CUFF and GRANT (1952)
	26	Fe (99.98%)	$Z - \sigma$	78,000	TAPSELL and CLENSHAW (1927)
28	Ni (98.7%)	$\epsilon - \theta$	65,400	HAZLETT, PARKER and NATHANS (1950)	
	Ni (99.5%)	$\theta_r - \sigma$	65,000	Battelle Memorial Institute	
29	Cu (pure)	$Z - \sigma$	44,000	NADAI and MANJOINE (1941)	
	Cu-Ni Solid Solution Alloy (45% Ni)	$Z - \sigma$	41,800	DUSHMAN, DUNBAR and HUTHSTEINER (1944)	
30	Zn (99.0%)	$\epsilon - \theta$ $Z - \sigma$	26,000	POMP and LANGE (1936)	
	Zn (99.99%)	$Z - \sigma$	26,000	GRAESER, HANEMANN and HOFMAN (1943)	
41	Nb (99.8%)	$\theta_r - \sigma$	75,000	GRASSI, BAINBRIDGE and HARMON (1951); ORR and BAINBRIDGE (1953)	
42	Mo	$\theta_r - \sigma$	120,000	PARKE (1951)	
	Mo-Nb (0.84% Nb)	$\theta_r - \sigma$	120,000	SEMCHYSHEN and HOSTETTER (1952)	
	Mo-V (0.87% V)	$\theta_r - \sigma$	120,000	SEMCHYSHEN and HOSTETTER (1952)	
48	Cd (99.96%)	$\epsilon - \theta$ $Z - \sigma$	22,000	FRENKEL (1954)	
		$\epsilon - \theta$ $Z - \sigma$	16,500	FRENKEL (1954)	
50	Sn (99.94%)	$\epsilon - \theta$ $Z - \sigma$	21,000	FRENKEL (1954)	
		$\epsilon - \theta$ $Z - \sigma$	56,000	CARREKER (1950)	
78	Pt (99.98%)	$\epsilon - \theta$	56,000	DUSHMAN, DUNBAR and HUTHSTEINER (1944)	
	Pt (pure)	$Z - \sigma$	56,000	DUSHMAN, DUNBAR and HUTHSTEINER (1944)	
79	Au (pure)	$Z - \sigma$	50,000	ALEXANDER, DAWSON and KING (1951)	
82	Pb (99.9998%)	$\epsilon - \theta$ $Z - \sigma$	19,000	SMITH (1941)	
		$\epsilon - \theta$ $Z - \sigma$	19,000	McKEOWN (1937)	
	Pb (99.997%)	$\epsilon - \theta$ $Z - \sigma$	19,000	McKEOWN (1937)	
		$Z - \sigma$	23,000	SMITH and HOWE (1945)	

TABLE 2.
Data on Activation Energies for Self-Diffusion of Metals*

Metal Atomic No.	ΔH self-diffusion, cal. per mol		Remarks (Data are for Polycrystals unless otherwise noted)
	Reported Values (Source Indicated)	Best or Average Value	
Lithium (8)	9,800 (a)	9,500	Deduced from nuclear resonance data
	9,800 (b)		Deduced from electrical resistance data
Carbon (6)	114,000 (c)	114,000	
Sodium (11)	10,450 (d)	10,450	Deduced from nuclear resonance data
	9,500 (e)		Deduced from electrical resistance data
	9,100 (b)		
Aluminium (18)	88,000 (f)	88,000	Estimated from diffusion data of other metals in aluminium
Potassium (19)	9,100 (b)	9,100	Deduced from electrical resistance data
α -Iron (26)	77,200 (g)	78,000	Extensive data, 720° to 900°C 800° to 900°C
	78,200 (h)		
	59,700 (i)		
γ -Iron (26)	48,000 (g)	71,000	Superseded by later work (h)
	74,200 (h)		
	67,900 (i)		
Cobalt (27)	67,000 (j)	75,000	
	61,900 (k)		
Copper (29)	45,100 (l)	48,000	Single crystal
	49,000 (l)		
	46,800 (m)		
	44,000 (n)		Based on diffusion data for copper in copper alloys extrapolated to zero concentration of alloying element
	57,200 (o)		
	61,400 (p)		Incomplete work, based on complete data at two temperatures only
Zinc (30)	47,000 (f)	20,400	Based on reinterpretation of published data
	20,400 (q)		Single crystal, $\Delta H/TC$ used in correlations with creep data
Silver (47)	81,000 (q)	46,000	Large grained polycrystals
	45,950 (r)		Single crystal
	45,950 (s)		Large grained polycrystals
	45,500 (t)		Based on reinterpretation of published data
	46,000 (f)		

*Note added in proof: SHEWNON and RHINNES, A.I.M.M.E., 1954 have determined the activation energy for self-diffusion in Mg (12) to be 82,000 cal/mole.

TABLE 2.—continued.
Data on Activation Energies for Self-Diffusion of Metals

Metal Atomic No.	ΔH Self-Diffusion, cal per mol		Remarks (Data are for Polycrystals unless otherwise noted)
	Reported Values (Source Indicated)	Best or Average Value	
Cadmium (49)	18,900 ₁ C (u) 17,800 ₁ C (u)	17,800	Single crystal, ΔH_{1C} used in correlations with creep data
Indium (49)	17,900 (v)	17,900	
Tin (50)	10,500 ₁ C (w) 5,900 ₁ la (w)	5,900	Single crystal, ΔH_{1la} used in correlations with creep data
Tungsten (74)	140,000 (x)	140,000	Diffusion of Fe in W extrapolated to 100 pct. W
Gold (79)	51,000 (y) 62,900 (z) 53,000 (a')	52,000	Extensive data, 721° to 966°C Data at three temperatures only
Lead (82)	27,900 (b') 27,000 (f)	28,000	Single crystal Based on reinterpretation of published data
Bismuth (88)	81,000 ₁ C(c') 140,000 ₁ C(c')	81,000	Single crystal, ΔH_{1C} used in correlations with creep data

- (a) H. S. GUTOWSKY and B. R. MCGARVEY : *J. Appl. Phys.* 1952 20, p. 1472.
 (b) D. K. C. MACDONALD : *J. Chem. Phys.* 1953 21, pp. 177-178.
 (c) L. GREEN, JR. : *J. Appl. Mech.* 1952 19, pp. 320-326.
 (d) N. H. NACHTRIEB, E. CATALANO and J. A. WEIL : *J. Chem. Phys.* 1952 20, pp. 1185-1188.
 (e) H. S. GUTOWSKY : *Phys. Rev.* 1951 83, p. 1073.
 (f) A. S. NOWICK : *J. Appl. Phys.* 1951 22, pp. 1182-1186.
 (g) C. E. BIRCHENALL and R. F. MEHL : *J. Appl. Phys.* 1948 19, p. 217.
 (h) C. E. BIRCHENALL and R. F. MEHL : *Trans. AIME* 1950 188, pp. 144-149 ; *J. Metals* (January 1950).
 (i) F. S. BUFFINGTON, I. D. BAKALAR and M. COHEN : *Trans. AIME* 1950 188, pp. 1874-1875 ; *J. Metals* (November 1950).
 (j) F. C. NIX and F. E. JAUMOT, JR. : *Phys. Rev.* 1951 82, pp. 72-74.
 (k) R. C. RUDER and C. E. BIRCHENALL : *Trans. AIME* 1951 191, pp. 142-146 ; *J. Metals* (February 1951).
 (l) M. S. MAIER and H. R. NELSON : *Trans. AIME* 1942 147, pp. 39-47.
 (m) C. L. RAYNOR, L. THOMASSEN and L. J. ROUSE : *Trans. ASM* 1942 30, pp. 818-825.
 (n) R. N. RHINES and R. F. MEHL : *Trans. AIME* 1938 128, pp. 185-221.
 (o) J. STEIGMAN, W. SHOCKLEY and F. C. NIX : *Phys. Rev.* 1939 56, pp. 13-21.
 (p) B. V. ROLLIN : *Phys. Rev.* 1939 55, p. 231.
 (q) P. H. MILLER, JR. and F. R. BANKS : *Phys. Rev.* 1942 61, pp. 648-652.
 (r) W. A. JOHNSON : *Trans. AIME* 1941 143, pp. 107-111.
 (s) R. E. HOFFMAN and D. TURNBULL : *J. Appl. Phys.* 1951 22, pp. 634-639.
 (t) L. SLIFKIN, D. LAZARUS and T. TOMIZUKA : *J. Appl. Phys.* 1952 23, pp. 1082-1088.

- (u) H. B. HUNTINGTON, J. S. SHIRN and E. S. WAJDA : *Anisotropic Diffusion*, Rensselaer Polytechnic Institute, Troy, New York, Progress Report No. 2, July 1, 1953.
 (v) R. E. ECKERT and H. G. DRICKAMER : *J. Chem. Phys.* 1952 20, pp. 18-17.
 (w) P. J. FENSHAM : *Australian J. Sci. Res.* 1950 3A, pp. 91-104.
 (x) J. A. M. VAN LIEMPT : *Rec. Trav. Chim.* 1945 64, pp. 239-249.
 (y) H. A. C. MCKAY : *Trans. Faraday Soc.* 1938 34, pp. 845-849.
 (z) A. M. SAGRUBSKIJ : *Phys. Zeit. Sowjet Union* 1937 12, pp. 118-119.
 (a') A. M. SAGRUBSKIJ : *Bull. Acad. Sci. U.S.S.R.* 1937 p. 903.
 (b') G. VON HEVESY, W. SEITH and A. KEIL : *Ztsch. Physik.* 1932 79, pp. 197-202.
 (c') W. SEITH : *Ztsch. Elektrochem.* 1933 39, pp. 538-542.

As outlined in Table 1 a complete survey was made (ORR, SHERBY and DORN 1954a ; 1954b) of creep and stress-rupture data on pure metals and binary solid solution alloys found to be sufficiently extensive for determination of the activation energy. In several cases approximately the same value of the activation energy for creep was obtained from data presented by different investigators using different

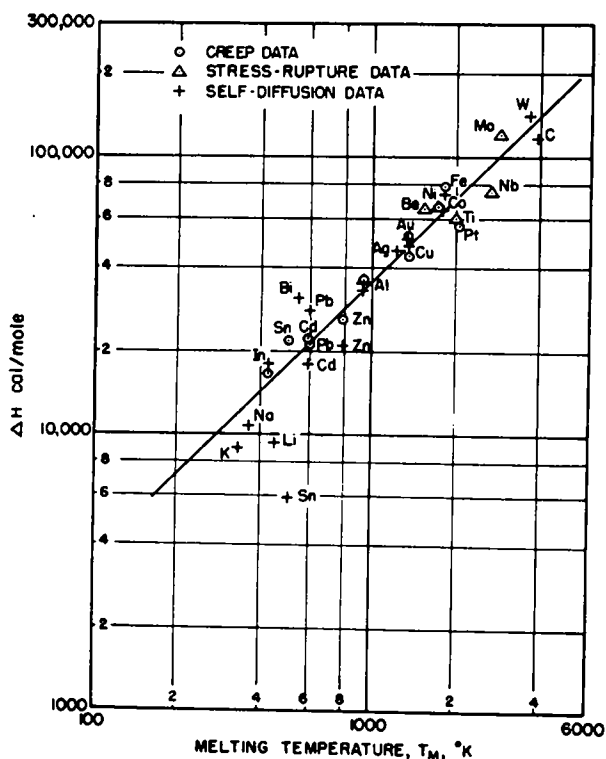


Fig. 15. Correlation of the activation energies for creep, stress-rupture and self-diffusion with the melting temperature.

purities and different pretreatments of the same base metal. In Table 2 are recorded the values of the activation energies for self-diffusion. As shown in Fig. 14, the activation energy for creep generally agrees well with that for self-diffusion. The Sn data deviate most seriously from the general correlation. As shown in Fig. 15, however, the activation energy for self-diffusion of Sn does not

correlate well with the usual trends of increasing activation energies for self-diffusion or creep with melting temperature, whereas the activation energy for creep of Sn coincides well with the general pattern. This suggests that despite the care that was exercised, some error might nevertheless have intruded into the evaluation of the activation energy for self-diffusion of Sn.

Neglecting the obviously important factor of crystal structure, some insight into the creep resistance of the elements might be gained by reviewing the periodic variation of the activation energies for creep and self-diffusion with atomic number as shown in Fig. 16. These empirical trends suggest that the highest creep resistant

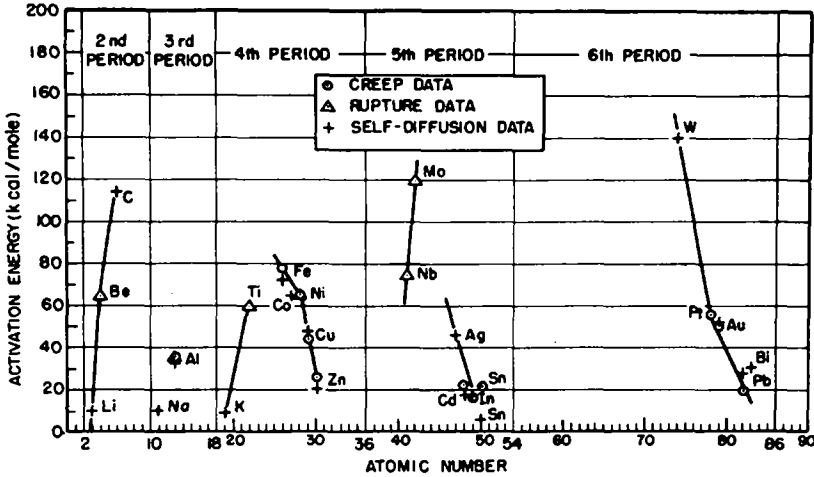


Fig. 16. Correlation of the activation energies for creep, rupture and self-diffusion with atomic number.

metals occur among those transition elements which exhibit the highest activation energies namely *W*, *Mo* and perhaps *V* in each series. Of course, as shown by the data of Fig. 18, a high activation energy is not the only factor responsible for high creep resistance. In fact introduction of minor alloying elements and stable dispersions also serve to improve the creep resistance even when the activation energy remains unaltered.

The apparent identity of the activation energy for creep with that for self-diffusion does not mean that high temperature creep is due to self-diffusion. But this apparent identity infers that the rate-controlling process for high temperature creep might be that of self-diffusion. Assuming that self-diffusion occurs by atom-vacancy interchanges, the activation energy for self-diffusion should arise from two terms. According to the Boltzmann distribution the number of vacancies in thermal equilibrium with the metal lattice should be proportional to $e^{-W/kT}$ where W is the energy required to produce a vacancy. If E be the activation energy for a vacancy-atom interchange, the frequency of such interchanges will be proportional to $e^{-E/kT}$. Consequently the activation energy for self-diffusion becomes $\Delta H = NW + NE$ per mole where N is Avogadro's number. (A similar expression applies for interstitial diffusion where W is the energy to produce an interstitial atom.) Since the activation energy for high temperature creep appears to agree

with that for self-diffusion, the number of vacancies participating in the rate-controlling self-diffusion process during creep must closely approximate the equilibrium number. This observation suggests that such excess vacancies (or interstitials) which are believed to be generated by Seitz's types of mechanisms (SEITZ 1952) are rapidly eliminated during high temperature creep.

Most formal theories of creep (KAUZMAN 1941 ; NOWICK and MACKLIN 1947) are predicted on thermal activation of dislocations over free energy barriers. As demanded by reaction rate theory, the creep rate for such processes give relations of the type

$$\dot{\epsilon} = Ae^{-\Delta H/RT} \sinh \left(\frac{V\sigma}{2kT} \right) \quad (8)$$

where A and V and ΔH might be taken as structure-sensitive parameters. Here the stress enters the equation for creep as a function of σ/T . But the observed $\epsilon - \theta$, $Z - \sigma$ and $\theta_r - \sigma$ relations all contain the stress and not σ/T as the appropriate variable for correlation. More conclusive evidence for the belief that stress alone and not σ/T enters the creep relationship will be presented in the following section. These observations suggest then that high temperature creep does not take place by thermal activation of dislocations over a barrier.

If high temperature creep were due to thermal activation of dislocations over a barrier it would be reasonable to expect ΔH to increase with increased barrier strengths introduced during creep or as a result of previous cold work. The constancy of ΔH with creep strain and cold work therefore support the hypothesis that high temperature creep does not involve thermal activation of dislocations over a free energy barrier.

Since high temperature creep is a continuing process, dislocations must either surmount barriers or move around barriers. Surmounting barriers by thermal activation does not, at present, appear to be a process that coincides deductions based on experimental observation. On the other hand as suggested by MOTT (1951, 1953) dislocations arrested at a barrier might undertake a climb process involving self-diffusion until they move to a plane where the barrier strength is equal to the applied stress. Under these conditions the dislocations would then circulate around the barrier. Thus the activation energy for high temperature creep could well be that for self-diffusion and the stress might enter the creep relationship as stress alone and not as σ/T .

5. GRAIN BOUNDARY SHEARING

In view of the complexity of the various processes occurring during creep of polycrystalline aggregates, it is somewhat surprising that creep can be correlated by such a simple functional relationship as that given by (1). In a series of unique investigations McLEAN (1951-1952 ; 1952-1953a, b, c) has shown that creep of polycrystalline aggregates occurs by means of migration of dislocations (resulting in slip and subgrain tilting) and by means of grain boundary shearing. Under a given stress the ratio of the fraction of the creep strain arising from grain boundary shearing to the total creep strain, $\epsilon_{g.b.}/\epsilon$, remains essentially constant. But this ratio increases as the stress decreases. Using McLEAN's techniques, the effect of temperature on grain boundary shearing was evaluated (FAZAN, SHERBY and

DORN) as recorded by the data in Table 3 for a constant load of 250 psi. The approximately constant values of $\epsilon_{g.b.}/\epsilon$ again confirm McLEAN's observations. Furthermore the same values of $\epsilon_{g.b.}$ were obtained at the same values of ϵ independent of the test temperature. Consequently, within the limits of experimental error, the same θ parameter and the same value of ΔH applies to grain boundary shearing as to the total creep strain. Consequently (1) is shown to be applicable to grain boundary shearing as well as to the total creep strain.

TABLE 3.
Results on Grain Boundary Shearing in High Purity Aluminium under 250 psi (FAZAN, SHERBY and DORN).

Temp. °K	Time Hours	ϵ	$\epsilon_{g.b.}$	$\epsilon_{g.b.}/\epsilon$	ΔH cal/mole
610	9.7	0.087	0.0035	0.095	38,500
747	0.029	0.087	0.0031	0.085	
610	20.4	0.07	0.0055	0.079	35,000
747	0.105	0.07	0.0051	0.073	
610	55.5	0.11	0.0085	0.076	38,000
640	14.42	0.11	0.0071	0.065	
700	1.215	0.11	0.0071	0.065	
747	0.15	0.11	0.0075	0.068	

The fact that the activation energy for grain boundary shearing is practically identical with that for the total creep strain suggests that grain boundary shearing might be attributed to localized crystallographic mechanisms of deformation in the vicinity of the grain boundary, rather than such a process as viscous shearing. This hypothesis is further substantiated by the fact that $\epsilon_{g.b.}/\epsilon$ is constant for creep at a given stress. Consequently, as demonstrated by McLEAN, the shape of the $\epsilon_{g.b.} - t$ curve is similar to that of the $\epsilon - t$ curve, suggesting that the same structural changes serve to decrease the rate of grain boundary shearing as operate to reduce the creep rate over the primary stage of creep. If grain boundary shearing were attributable to viscous flow $\epsilon_{g.b.}$ would have been a linear function of t and the ratio $\epsilon_{g.b.}/\epsilon$ should have increased with ϵ .

Since $\epsilon_{g.b.}$ is a function of θ for a given stress, independent of temperature, the localized strain damage in and about the grain boundary region, such as might lead to intergranular fracturing, should also depend on θ independent of the temperature. Such independence of the temperature suggests that the "so-called" equicohesive temperature (below which failures are transcrystalline and above which they are intergranular) might be a highly fictional concept. McLEAN's data, which reveal that the ratio of $\epsilon_{g.b.}/\epsilon$ increases as the stress is decreased, suggest that the strain damage becomes concentrated more and more in the vicinity of the grain boundary as the stress is reduced. Perhaps future investigations will more conclusively reveal that "so-called" intergranular fracturing occurs below some critical stress rather than above some critical temperature.

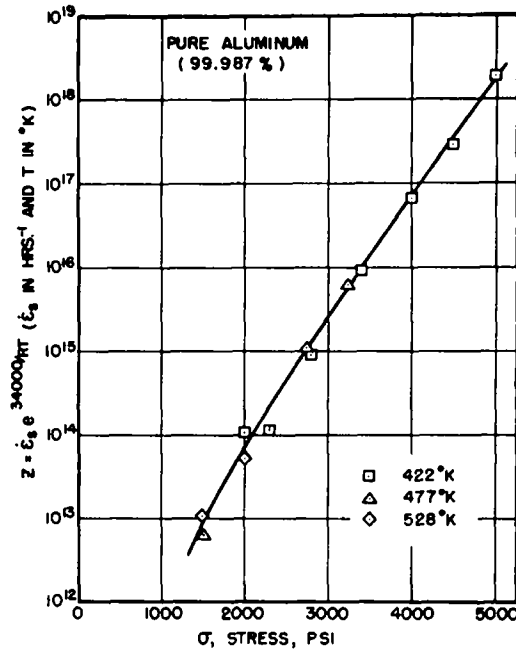


Fig. 17. Effect of stress on the Zener-Hollomon parameter for secondary creep. (Data of SHERBY and DORN 1953).

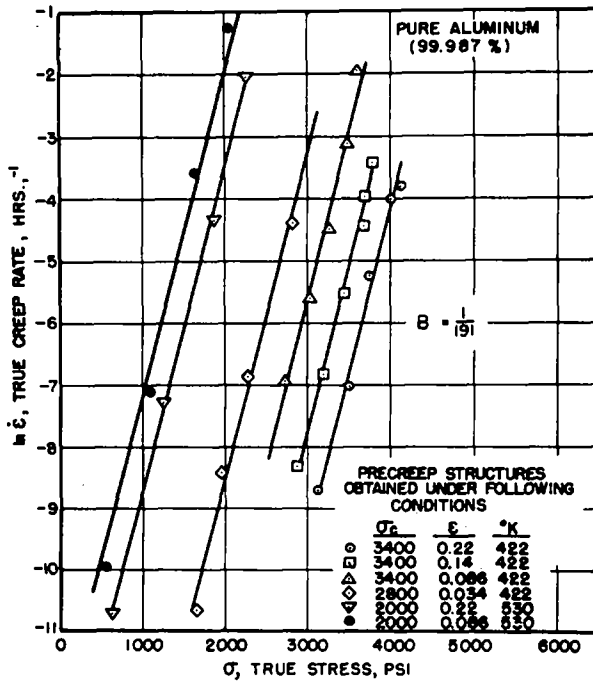


Fig. 18. Effect of stress on the creep rate for a constant structures (Data of SHERBY, FRENKEL, NADEAU and DORN 1954).

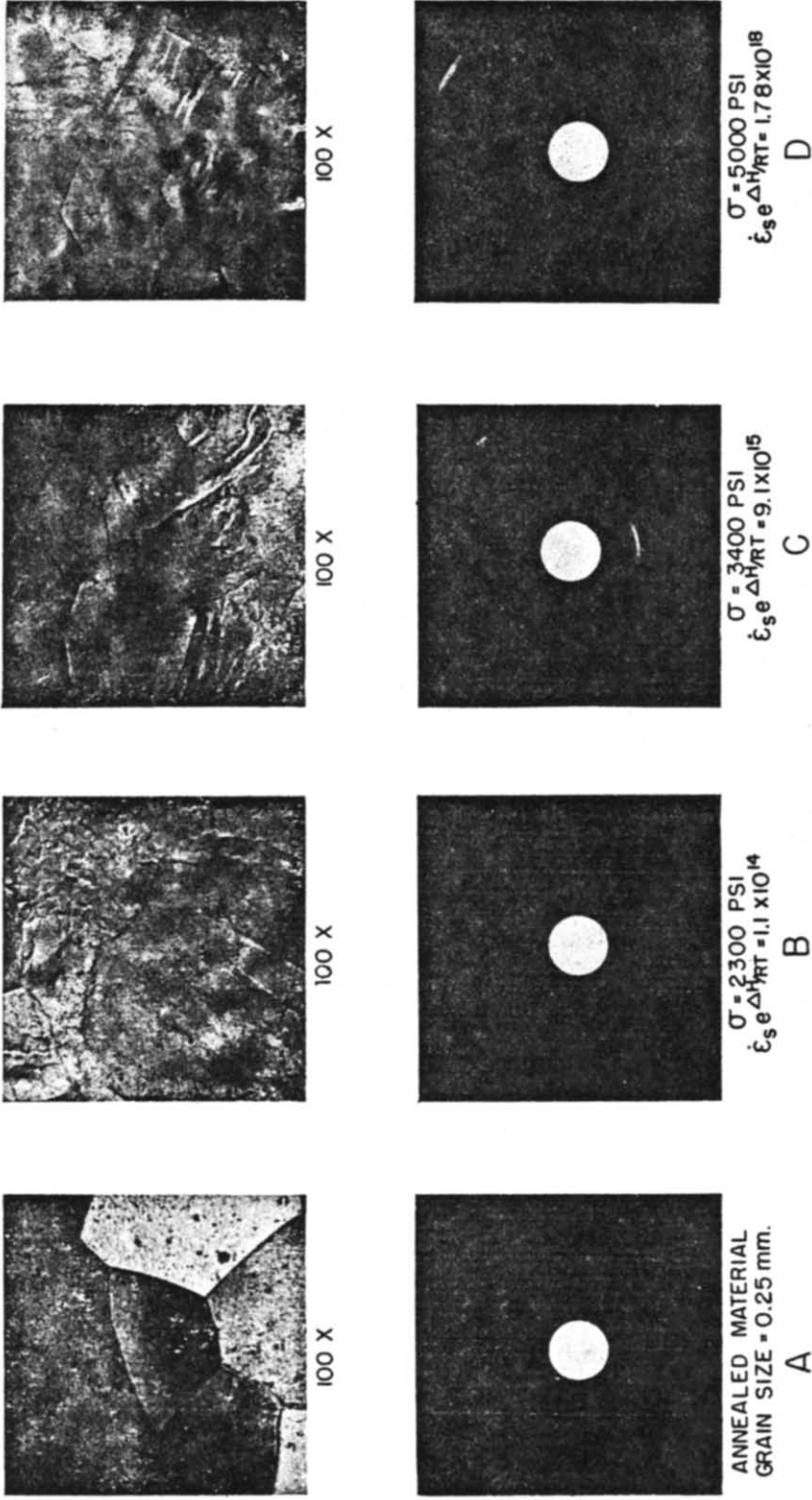
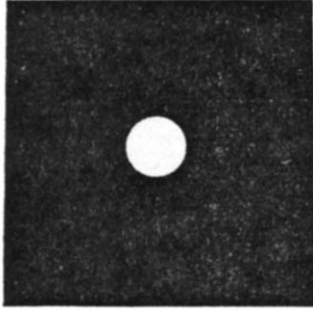
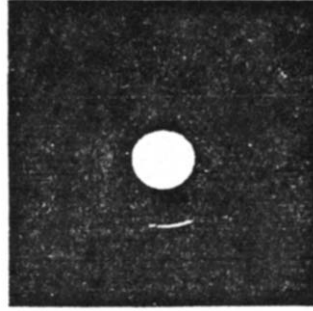


Fig. 19. Metallographic and X-ray photographs of creep specimens of high purity aluminum as a function of the parameter (SHERBY and DORN 1953).

ANNEALED ALUMINUM

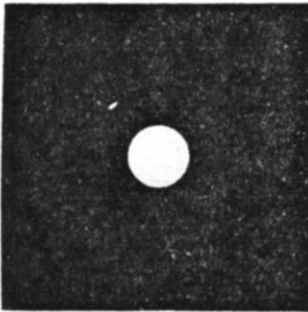


A. BEFORE CREEP TESTING.

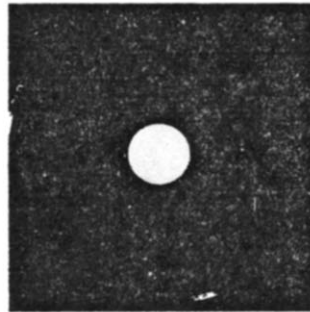


B. AT FRACTURE AFTER CREEP UNDER $\sigma_c = 3400$ PSI AT 477°K .

ANNEALED ALUMINUM PRESTRAINED 15% AT 78°K AND RECOVERED TO $\theta_R = 8.386 \times 10^{-17}$



A. BEFORE CREEP TESTING.



B. AT FRACTURE AFTER CREEP UNDER $\sigma_c = 3400$ PSI AT 477°K .

Fig. 20. X-ray back reflection photographs of annealed and worked aluminium before and after creep testing (FRENKEL, SHERBY and DORN 1953).

6. STRESS LAW FOR CREEP

Many attempts have been made to determine the effect of stress on creep. In general this has been done by determining the effect of stress on the secondary creep rate, as shown by the $Z - \sigma$ data presented in Fig. 17. Although, as previously described, the same structure is obtained during secondary creep at the same stress independent of the test temperature, a systematic sequence of different structures are developed as a function of stress. Thus as shown by the back-reflection Debye-Scherrer diagrams and photomicrographs of Fig. 19, the $Z - \sigma$ data of Fig. 17 reflect not only the effect of stress but also the effect of structural differences on the creep rate.

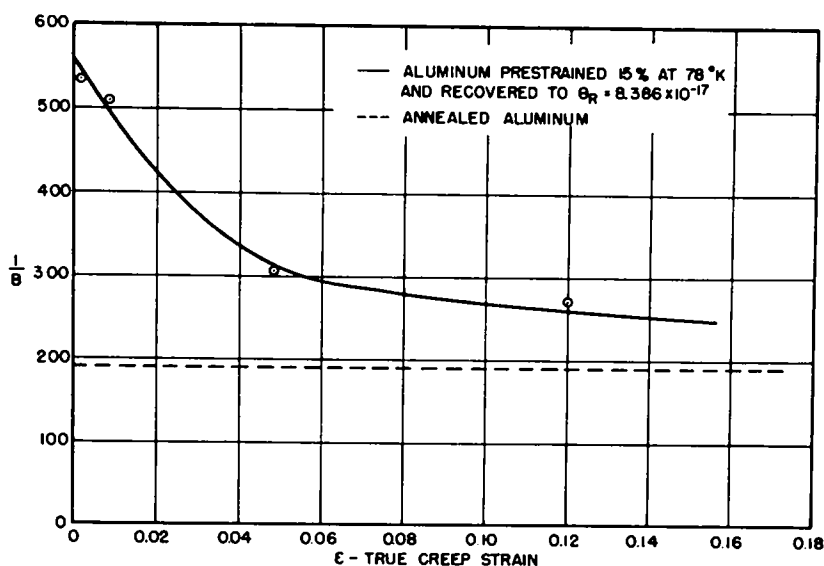


Fig. 21. Effect of creep on $1/B$ for cold-worked aluminium under a constant load of 4,000 psi at 447°K. (Data of FRENKEL, SHERBY and DORN 1953).

The stress law for creep can be isolated only by employing test procedures that permit the evaluation of the effect of stress on the creep rate for the same structure. Preliminary tests (SHERBY, FRENKEL, NADEAU and DORN 1954) having this objective in mind were conducted by prestraining a series of specimens under the same constant load to the same strain and then reducing the true stress to a series of lower values. Following the drop in true stress the instantaneous creep rate was determined as a function of the new true stress. Inasmuch as each specimen of the series was crept the same amount under the same load, each specimen had the same structure developed in it at the instant the stress was reduced. Increasing the stress was avoided because the instantaneous creep strain introduced upon increase of the stress would have modified the structure in a way dependent upon the magnitude of the adjusted stress. When the natural logarithm of the instantaneous creep rate was plotted as a function of the stress, the linear correlation illustrated in Fig. 18 was obtained. These data reveal that

$$\dot{\epsilon} = Ae^{B\sigma} \quad (9)$$

where B is the slope of the $\ln \dot{\epsilon} - \sigma$ plot. In general B appears to be approximately constant, independent of the precreep conditions of loads or strains. Since the structure generated during creep is dependent on the precreep conditions of load and strain, it follows that B is insensitive to the structural changes attending the creep of initially annealed metals. Furthermore, the data of Fig. 9 reveal that B is insensitive to the test temperature. Therefore the creep rate following a decrease in stress can be correlated by

$$\dot{\epsilon} = S' e^{-\Delta H/RT} e^{B\sigma} \quad (10)$$

where, within the limits of experimental error, ΔH and B are substantially constant for a given material. Thus S' is the only-structure sensitive parameter of (10).

Although B is insensitive to the structural changes occurring during high temperature creep of annealed specimens, it is sensitive to cold work (FRENKEL, SHERBY and DORN 1958). The back-reflection Debye-Scherrer X-ray photograms of Fig. 20 reveal in part the structural modifications introduced in a cold worked and partially recovered specimen of aluminium. The $1/B$ values from such initially cold worked and partially recovered specimens are given by the data of Fig. 21. Thus cold working increases $1/B$ and the $1/B$ value changes during subsequent creep, finally approaching the value appropriate for that obtained from an initially annealed specimen. The X-ray photograms of Fig. 20 reveal that almost identical subgrain structures are obtained following extensive creep under identical conditions, independent of the initial state of the material. As shown in Fig. 22, $1/B$ increases almost linearly with the atomic percent of alpha solid solution alloying additions.

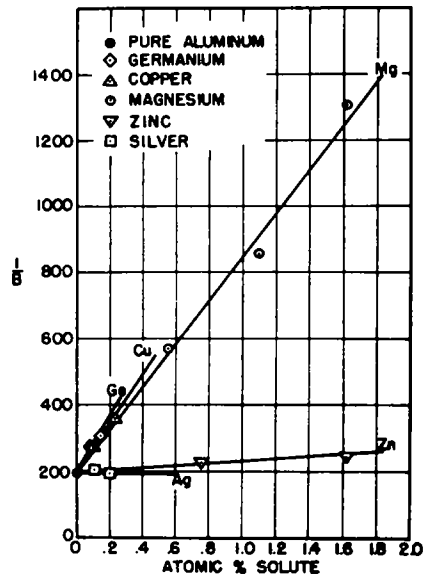


Fig. 22. Effects of alloying elements of the parameter $1/B$ for creep. (Data of SHERBY, FRENKEL, NADEAU and DORN 1954).

Obviously (10) cannot be valid for low stresses since $\dot{\epsilon}$ must vanish as σ approaches zero. A new series of investigations were therefore conducted (LAKS 1953) to ascertain what the stress law for creep might be at very low stresses. If the applied stresses are sufficiently low, the initial creep strain is zero, as shown in Fig. 23, and the initial creep rate is therefore that appropriate to the annealed state. The linear relationship that was obtained between the logarithm of the initial creep rate and the logarithm of the true stress, as shown in Fig. 24, suggests that over the low range of stresses

$$\dot{\epsilon} = S'' e^{-\Delta H/RT} \sigma^n \quad (11)$$

Additional confirmation of the nominal validity of this relationship is contained in the low stress-zero initial creep strain data for a series of alpha solid solutions

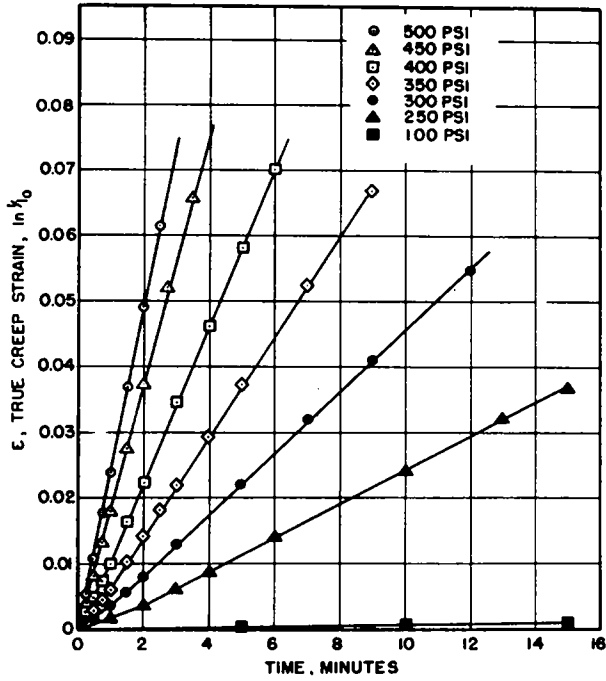


Fig. 23. Constant load creep of aluminium containing 3.1 atomic percent magnesium at low stresses. (Data of H. LAKS 1953).

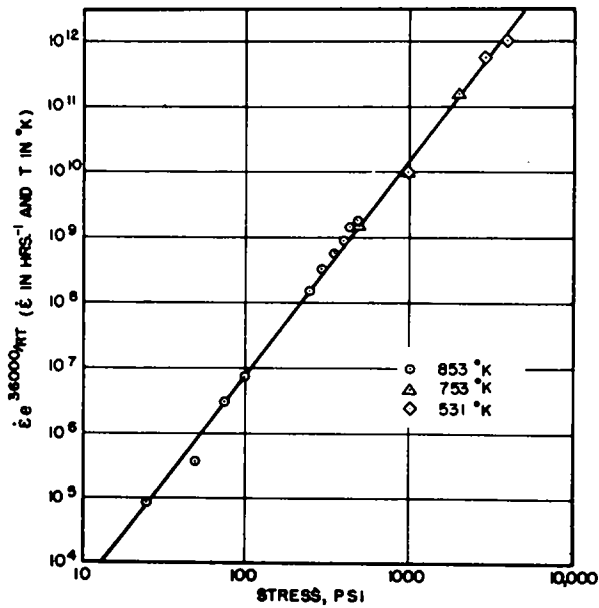


Fig. 24. Effect of small stresses on the creep rate of aluminium containing 3.1 atomic percent magnesium. (Data of H. LAKS 1953).

of Mg in Al shown in Fig. 25. These data reveal that n of (11) decreases with increasing amounts of alloying whereas S'' for the annealed state is practically independent of alloying.

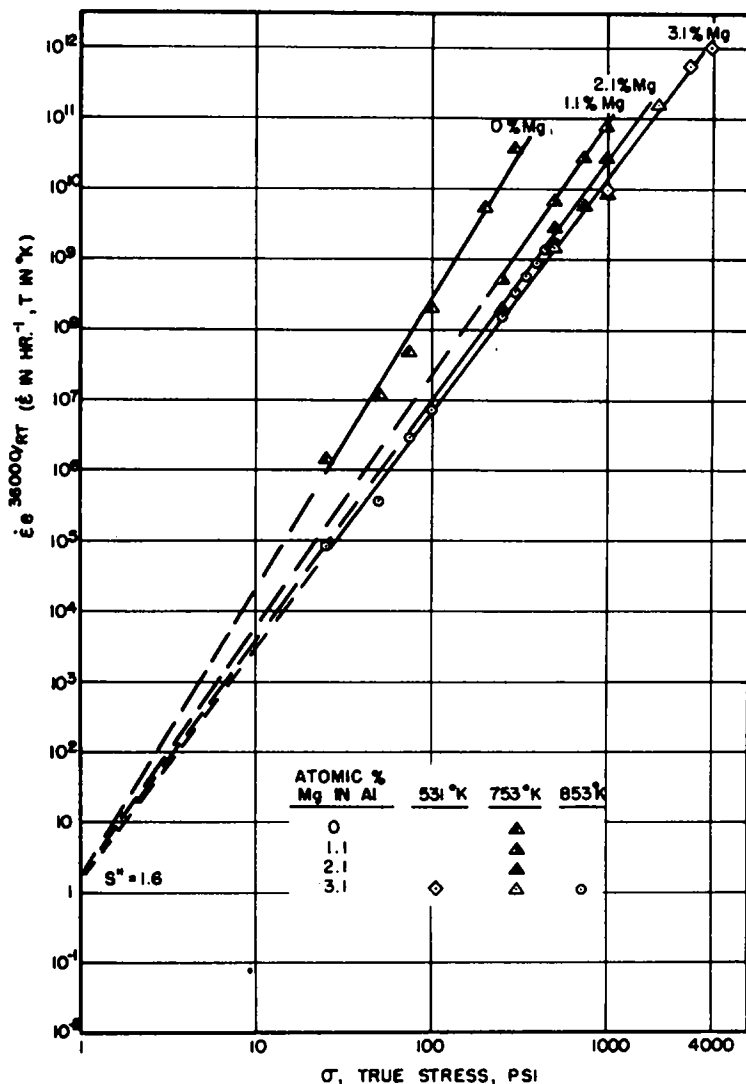


Fig. 25. Effect of solid solution alloying on the initial rate at low stresses.

It is indeed rational to suspect that the high and low stress creep laws defined by (10) and (11) are in no way due to any abrupt change in the mechanism of creep and therefore merely reflect two limiting conditions of a single law for creep. A preliminary test of this hypothesis was obtained by precreeping a series of specimens of aluminium containing 3.1 atomic percent magnesium to a strain of 0.077 at a constant load of 10,000 psi and at 531°K following which the new initial creep rates at various reduced stresses were obtained. As shown by cut A

of Fig. 26 the creep rate is proportional to $e^{B\sigma}$ at high stresses whereas cut B of Fig. 26 reveals that it is proportional to σ^n at low stresses under otherwise identical conditions of test. Thus it appears possible to generalize (10) and (11) to read

$$\dot{\epsilon} = S e^{-\Delta H/RT} \phi(\sigma) \tag{12}$$

where

$$S \phi(\sigma) = S' e^{B\sigma} \text{ for high stresses, and}$$

$$S \phi(\sigma) = S'' \sigma^n \text{ for low stresses.}$$

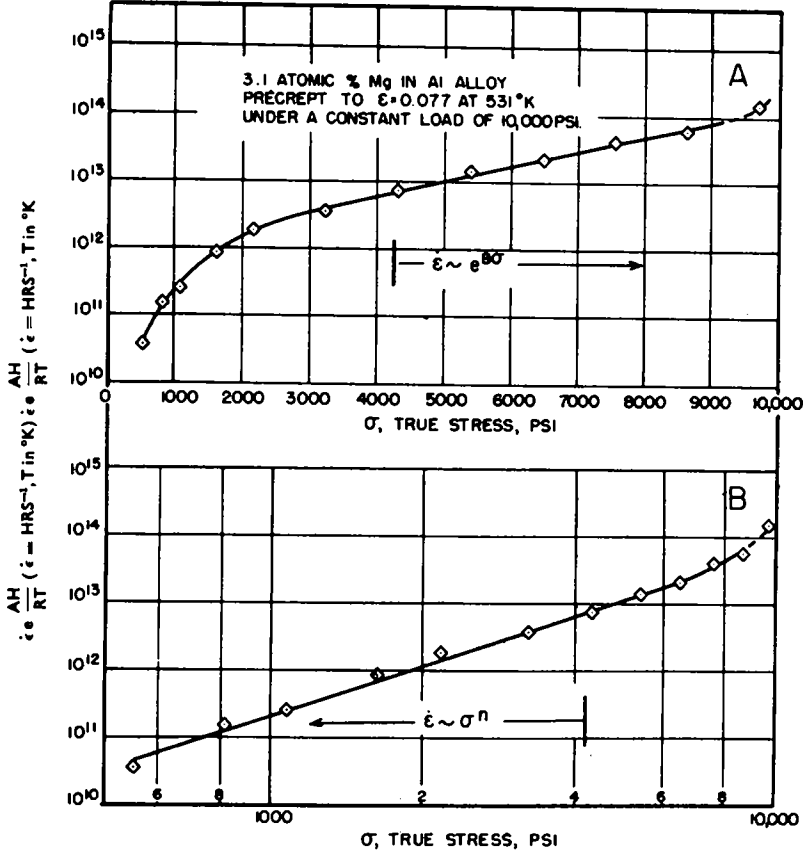


Fig. 26. Effect of stress on the creep rate for the same structure.

Additional confirmation of this hypothesis is also contained by the data recorded in Fig. 27. For alloys exhibiting vastly dissimilar values of B the transition from $e^{B\sigma}$ to σ^n types of laws should occur at the same values of the total argument $B\sigma$, if a single function exists. The data of Fig. 27 reveal that the high stress creep law is valid above about $B\sigma = 1.4$ independent of the value of B .

7. TRANSIENT PHENOMENA

The observations made above suggest that the law for high temperature creep of annealed simple metallic systems might now be fairly simply formulated in

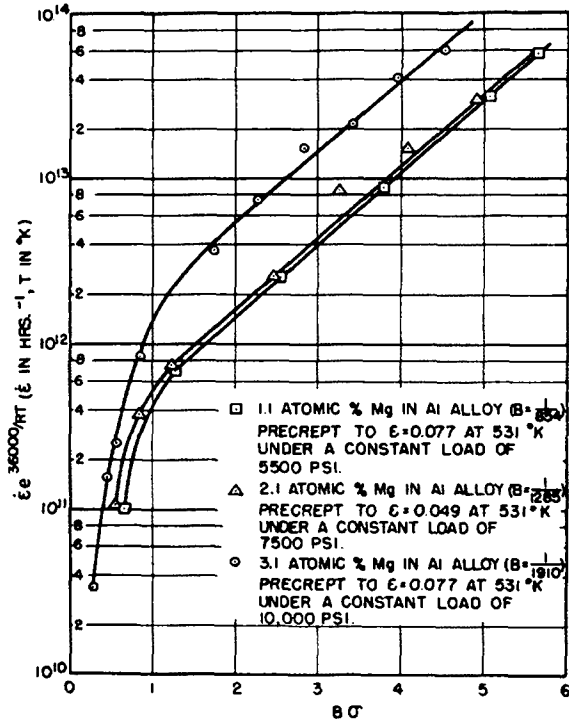


Fig. 27. Range of validity of high stress creep law in terms of σ .

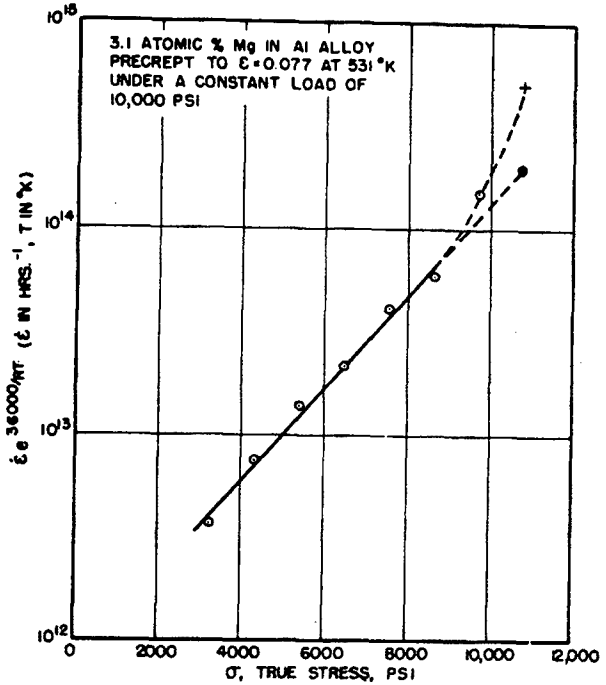


Fig. 28. Failure of $\dot{\epsilon} e^{B\sigma}$ relationship for small decreases in stress.

terms of (12) where S is the major structure-sensitive parameter. This, however, is not true and much yet remains to be done to clarify some of the details of creep phenomena. In fact it is some of these details which might eventually lead to a more complete understanding of the phenomenon of high temperature creep.

For example (10) was found to be valid for the initial creep strain rate following reduction of the original creep stress. But it is not yet certain that it applies rigorously to the original creep process preceding reduction in stress. In fact the typical example given in Fig. 28 strongly suggests that the linear $\ln \dot{\epsilon}$ versus σ curve does not include the last point on the original creep curve (shown by +) just preceding the time the stress was decreased. The discrepancy between the actual datum and the extrapolated value (shown by \oplus) increases as the original creep stress increases. Inasmuch as the structure must be identical immediately preceding and immediately following a decrease in stress, the reason for this

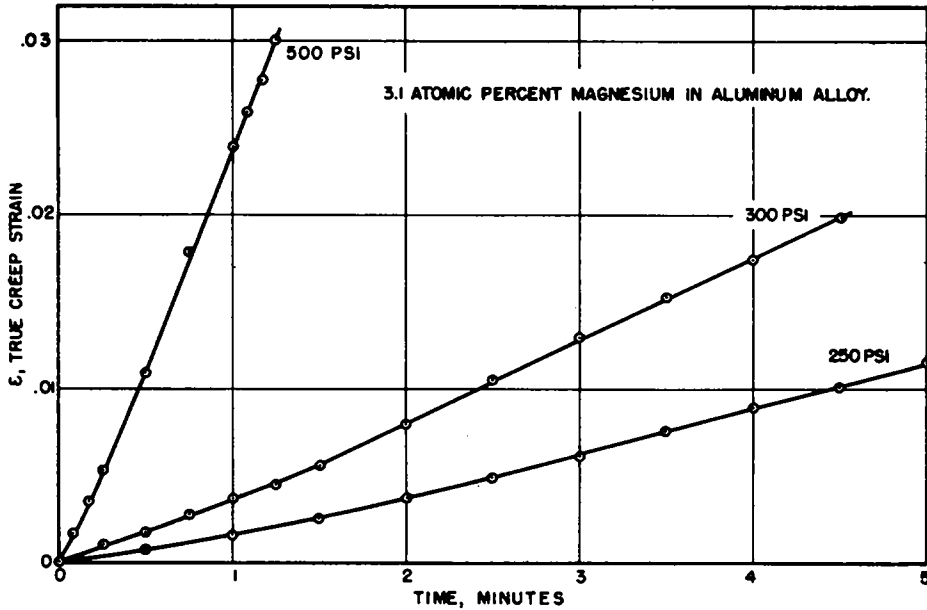


Fig. 29.

somewhat anomalous observation is not readily resolved. It is possible that as the creep stress is decreased only slightly, more barriers of lower strengths become effective in blocking the motion of dislocations thus decreasing the creep rate more rapidly than prescribed by the $e^{B\sigma}$ law. This should continue until the newly applied stress drops below the strength of the weakest barrier. Any additional decrease in stress would no longer cause any additional change in the pattern of effective barriers and therefore for all lower stresses the same stress law, namely $e^{B\sigma}$ or σ^n might apply.

It appears quite definite that an initial creep rate is obtained immediately upon applying the stress even at very low stress (as low as 10 psi). It is this initial creep rate that was used in establishing (11). But over the initial portion of the creep curve this rate increases and reaches a steady-state creep rate before

it exhibits the usual trend of decreasing creep rates over the primary stage. Typical examples of this behaviour are recorded in Fig. 29.

This behaviour might possibly be explained in terms of MOTT's model for high temperature creep (MOTT 1951). Dislocations begin to migrate immediately upon application of the stress. But if high temperature creep occurs primarily as a result of dislocation climb past barriers, some time interval will be required before a steady-state pattern of climbing dislocations can be established. Thus the initial creep rate should at first increase before the primary stage of decelerating creep rates is obtained.

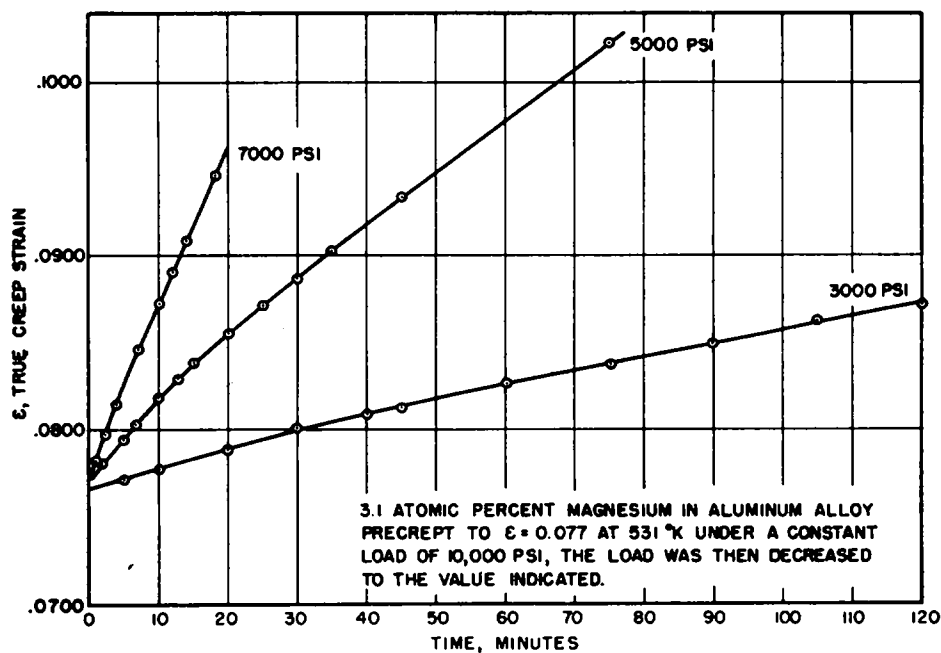


Fig. 80. Transients upon decreasing the stress.

Transients are also observed when the stress is decreased. But in the realm of high temperature creep under discussion here the transients are distinctly different from those previously reported by other investigators (CARREKER, LESCHEN and LUBAHN 1949; COTTRELL and AYTEKIN 1950). As shown by the typical examples of Fig. 80, the creep rate decreases with time following a drop in stress until some steady state is reached. This phenomenon cannot be explained by the crystal recovery mechanisms for transients at lower temperatures postulated by COTTRELL and AYTEKIN (1950) and also KUHLMANN (1951). or by the possible effects of creep recovery. It appears as if these observations might also be explained by MOTT's model for high temperature creep. Under the original high stress a large number of dislocations are in the process of climbing. Inasmuch as the climbing dislocations exist on a series of slip planes they cannot migrate back to their FRANK-READ sources immediately upon reduction of the stress. Consequently more than the steady-state number of dislocations for the new stress are climbing

to circumvent the barriers immediately following a reduction of stress. After an appropriate interval of time, however, the steady-state number for the new stress will be reached.

The two upper curves of Fig. 81 give the relationship between the estimated values of the instantaneous creep rate as well as the steady-state creep rate after the stress was reduced to the reported values. The difference between the instantaneous and steady-state creep rates is minor in the high stress range but it becomes

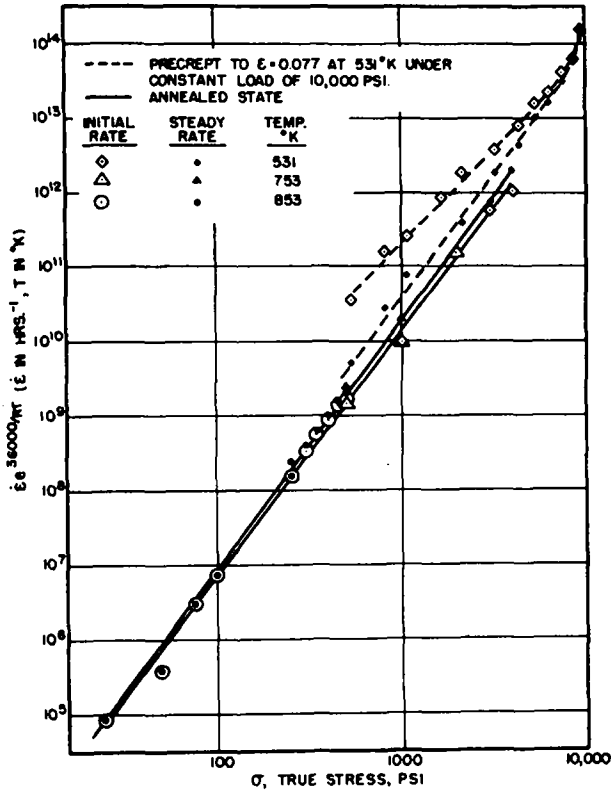


Fig. 81. Comparison of instantaneous and steady state creep rates.

pronounced at the lower stresses. Thus approximately the same values of B and S' are obtained for either the instantaneous or the steady-state creep rates. But in the range of lower stresses where the σ^n law applies n and S'' are quite different for the instantaneous and steady-state creep rates.

The two lower curves of Fig. 81 refer to the steady-state and instantaneous creep rates for the same material in the annealed state immediately following the first application of the stress. In this range the differences between the steady-state and instantaneous creep rates are small and increase only slightly with increase in stress. It may be significant to note that the steady-state value of n on decreasing the stress following precreep agrees well with the steady-state value of n upon first application of the stress, as evidenced by the parallelism between the $\ln \dot{\epsilon} e^{AH/RT}$ versus $\ln \sigma$ curves. This agreement in the values of n

for the two steady-state sets of data might have been anticipated inasmuch as the steady-state pattern of dislocations migrating past barriers are presumably the same at the same stress. The difference in the elevation of these curves, however, arises from the fact that S'' is different in the two cases due to the possibility that their patterns of barriers are dissimilar as a result of the dissimilar strain histories in each case.

8. CONCLUSIONS

1. High temperature creep of thermally stable alloys is correlatable by the functional relationship

$$\epsilon = f(\theta), \quad \sigma = \text{constant}$$

where ϵ = total creep strain

$$\theta = t e^{-\Delta H/RT}$$

t = duration of test

ΔH = activation energy for creep

R = gas constant

T = absolute temperature.

2. Grain boundary shearing obeys a similar functional relationship having the same activation energy.

3. The activation energy for high temperature creep approximates that for self-diffusion.

4. The stress appears to enter the high temperature creep law as σ and not as σ/T .

5. Conclusions 3 and 4 suggest that high temperature creep is not due to thermal activation of dislocations over a barrier but rather occurs as a result of dislocation climb by a self-diffusion process.

6. After an appropriate decrease in stress, the new creep rate is given by

$$\dot{\epsilon} = S e^{-\Delta H/RT} \phi(\sigma)$$

where S appears to depend on the barrier pattern and where

$$\phi(\sigma) \sim e^{B\sigma} \text{ at high stresses}$$

$$\phi(\sigma) \sim \sigma^n \text{ at low stresses.}$$

7. Transients encountered during changes in stress suggest that high temperature creep might be ascribed to a dislocation climb process.

ACKNOWLEDGMENTS

The author wishes to express his sincere appreciation to the Office of Naval Research for their wholehearted support of the investigations on high temperature creep reviewed here. The success of many of these studies were due to enthusiastic cooperation of several colleagues and numerous graduate students at the University of California. The author particularly wishes to acknowledge the substantial contributions made by his colleague, Mr. O. SHERBY, to this programme of investigation.

REFERENCES

- ALEXANDER, B. M., DAWSON, M. H.
and KLING, H. P. 1951 *J. Appl. Phys.*, **22**, 439-448.
- CARREKER, R. P., LESCHEN, J. G.
and LUBAHN, J. D. 1949 *Transactions, A.I.M.E.*, **180**, 139-146.
- CARREKER, R. P. 1950 *J. Appl. Phys.*, **21**, 1286-1296.
- COTTRELL, A. H. and AYTEKIN, V. 1950 *J. Inst. Metals*, **77**, 389-422.
- CUFF, F. B., Jr. and GRANT, N. J. 1953 *The Iron Age* **170**, 134-139.
- DUSHMAN, S., DUNBAR, L. W.
and HUTHSTEINER, H. H. 1944 *J. Appl. Phys.*, **15**, 108-124.
- FAZAN, B., SHERBY, O. D.
and DORN, J. E. — *AIME*, to be published in *Journal of Metals*.
- FRENKEL, R. E., SHERBY, O. D.
and DORN, J. E. 1953 Institute of Engineering Research Report, University of California, Berkeley, California, Series No. 22, Issue 29, August 1st.
- GIEDT, W. H., SHERBY, O. D.
and DORN, J. E. 1953 To be published in *Trans. ASME*.
- GRAESER, W., HANEMANN, H.
and HOFMANN, W. 1943 *Z. Metallkunde*, **35**, 1-13.
- GRASSI, R. C., BAINBRIDGE, D. W.
and HARMON, J. W. 1951 Institute of Engineering Research Report, University of California, Berkeley, Series No. 22, Issue No. 28, July 1st.
- GREENOUGH, G. B. and SMITH, EDNA 1950 *J. Inst. Metals*, **77**, 435-443.
- HAZLETT, T. H., PARKER, E. R.
and NATHANS, M. 1950 Institute of Engineering Research Report, University of California, Berkeley, Series No. 28, Issue No. 8.
- KAUFMAN, A. R., GORDON, P.
and LILLIE, D. W. 1950 *Trans. ASM.*, **42**, 785-844.
- KAUZMAN, W. 1941 *Trans. AIME.*, **143**, 57-83.
- KUHLMANN, D. 1951 *Proc. Phys. Soc.*, **64A**, 140-155.
- LAKS, H. 1953 M.S. Thesis, College of Engineering, University of California, Berkeley, California.
- McKEOWN, J. 1937 *J. Inst. Metals*, **60**, 201-228.
- McLEAN, D. 1951 *J. Inst. Metals*, **80**, 507-519.
1952 *J. Inst. Metals*, **81**, 133-144.
1952 *J. Inst. Metals*, **81**, 287-292.
1952 *J. Inst. Metals*, **81**, 293-300.
- MOTT, N. F. 1951 *Proc. Phys. Soc.*, **64**, 729-741.
- MOTT, N. F. 1953 *Phil. Mag.*, **44**, series 7, 742-765.
- NADAI, A. and MANJOINE, M. J. 1941 *Trans. ASME.*, **63**, A-77-A-91.
- NOWICK, A. S. and MACHLIN, E. S. 1947 *J. Appl. Phys.*, **18**, 79-87.
- ORR, R. L. and BAINBRIDGE, D. W. 1953 Institute of Engineering Research Report, University of California, Berkeley, Series No. 22, Issue No. 28, July 1st.
- ORR, R. L., SHERBY, O. D.
and DORN, J. E. 1954 *Trans. ASM.*, **46**.
- ORR, R. L., SHERBY, O. D.
and DORN, J. E. 1954 *J. Metals, AIME.*, 71-80.
- PARKE, R. M. 1951 *Met. Prog.*, **60**, No. 1, 81-96.
- POMP, A. and LANGE, W. 1936 *Mitt. Kaiser-Wilhelm Institute Eisenforschung Zu Dusseldorf*, **18**, 51-63.
- ROBERTS, C. S. 1953 *J. Metals, AIME*, 1121-1125; see discussion of paper by O. D. SHERBY and R. E. FRENKEL.

- SCHWOPE, A. D. Personal communication. Battelle Memorial Institute, Columbus, Ohio.
- SEITZ, R. and READ, T. A. 1941 *J. Appl. Phys.*, 12, 57-83.
- SEITZ, R. 1952 *Advances in Physics*, 1, 48-89.
- SEMCHYSHEN, M. and HOSTETTER, H. 1952 Third Annual Report, NR-034-401, Climax Molybdenum Company of Michigan.
- SERVI, I. S. and GRANT, N. J. 1951 *Trans. AIME.*, 191, 917-922.
- SERVI, I. S. and GRANT, N. J. 1951 *Trans. AIME.*, 191, 909-916.
- SHERBY, O. D. and DORN, J. E. 1952 *Trans. AIME*, 194, 959-964.
- SHERBY, O. D. and DORN, J. E. 1953 *J. Metals, AIME.*, 5, 324-330.
- SHERBY, O. D., FRENKEL, R.,
NADEAU, J. and DORN, J. E. 1954 *J. Metals, AIME.*, 275-279.
- SMITH, A. A., Jr. 1941 *Trans. AIME.*, 143, 165-171.
- SMITH, A. A., Jr. and HOWE, H. E. 1945 *Trans. AIME.*, 161, 472-477.
- TAFSELL, H. J. and
GLENSHAW, W. J. 1927 Great Britain Dept. of Science and Industrial Research, Special Report No. 1.
- WOOD, W. A. and WILMS, G. R. 1949 *J. Inst. Met.*, 75, 698-706.
- WOOD, W. A., WILMS, G. R.
and RACHINGER, W. A. 1949 *J. Inst. Metals*, 79, 159-172.
- WYON, G. and CRUSSARD, C. 1951 *Revue de Metallurgie*, 48 (2), 121-130.
- ZENER, C. and HOLLOMON, J. H. 1944 *Trans. ASM.*, 33, 163-235.
- ZENER, C. and HOLLOMON, J. H. 1944 *J. Appl. Phys.*, 15, 22-32.